Titanium-Containing Zeolites. A Periodic ab Initio Hartree−Fock Characterization

C. M. Zicovich-Wilson[†] and R. Dovesi*

Department of Inorganic, Physical and Materials Chemistry, University of Torino, via P. Giuria 5, I-10125 Torino, Italy

Received: July 17, 1997; In Final Form: November 3, 1997

The equilibrium geometry, electronic structure, and relative stability of titanozeolites have been investigated at an ab initio level by using the periodic quantum mechanical program CRYSTAL. Nine periodic crystalline models of composition $(TiO_2)_x$ $(SiO_2)_{1-x}$, with different framework type structures (chabazite, sodalite, and α-quartz) and values of x, have been considered. Rutile has also been considered as a TiO_2 reference system. The geometry of the various models has been fully optimized by using a split valence double-zeta basis set. The effect of more extended basis sets on the relative stabilities and electronic properties at the optimized geometry has been explored. Four-fold-coordinated titanium, as present in titanozeolites, is 17-24 kcal·mol^{-1} less stable than 6-fold-coordinated Ti in rutile, the actual value depending on the structure and composition of the models.

1. Introduction

Since the discovery of the unique catalytic properties of titanium silicalites, namely, TS-1 and TS-2,[1−3] in selective oxidative reactions using hydrogen peroxide, considerable effort has been devoted to the synthesis of similar materials with a variety of framework structures and selectivity behaviors. In recent years other Ti-containing zeolites have been prepared, including Ti-Beta (*BEA),[4,5] Ti-Y (FAU),[6] Ti-mordenite (MOR),[7] and also mesoporous silicates such as Ti-MCM-41,[8] ETS-10,[9] and Ti-HMS.[10]

Zeolitic frameworks are generated by combination of corner-shared TO_4 tetrahedra, where T is normally Si or Al, but other elements such as Ga, B, and Fe can also be introduced in the framework by direct hydrothermal synthesis or by postsynthesis isomorphous substitution.[11] From the three-dimensional organization of the tetrahedra, structures are obtained that present multidimensional channels and cavities.[12,13]

In the case of Ti-zeolites, strong evidence exists indicating that Ti atoms occupy intraframework 4-fold-coordinated positions.[2,14,15] The local structure and siting of Ti centers are however controversial, since experimental techniques usually adopted for the determination of local structures in solids, that is, X-ray diffraction and NMR, cannot give accurate information in this case, the reason being the low Ti content and crystallinity of the samples[16] in the first case and the large quadrupolar moment of the ^{47} Ti and ^{49} Ti isotopes[17] in the second. Only indirect characterization of the Ti sites is therefore possible, by means of EXAFS−XANES,[18−22] vibrational,[23−25] and electronic[2,18] spectroscopies. As Ti centers are supposed to be the active sites for oxidative reactions, accurate information on their local properties, such as geometry and electronic structure, is of fundamental importance for understanding the catalytic behavior of these compounds.

The aim of this study is to contribute to the accurate characterization of catalytic Ti centers in zeolites and silicates in general, by using ab initio quantum mechanical methods. The periodic Hartree−Fock (PHF) scheme as implemented in the CRYSTAL code[26,27] has been employed, which provides the electronic ground-state energy and wave function for a crystalline material subject to periodic boundary conditions. The periodic approach permits one to avoid undesirable border effects that are always present when cluster models are adopted for representing active sites of solid catalysts.[28]

In the last years, a few quantum mechanical calculations with the cluster approach have been reported, concerning Ti centers in zeolites. Millini et al.[29] and Jentys et al.[30] investigated geometries and relative stabilities of different Ti sites in TS-1. In the first case a density functional theory (DFT) scheme has been applied to geometry-constrained cluster models; in the second case a classical force field combined with a quantum mechanical cluster approach has been used. More recently, De Man and Sauer[31] performed Hartree−Fock calculations with molecular (cluster) models representing substructures of titanozeolites and titanosilicates that were compared with their pure silica analogues. Calculated energies, geometrical parameters, and vibrational spectra were used to discuss local features of active Ti centers in solid catalysts. The reactivity of Ti sites in oxidative reactions was recently explored by using also DFT schemes applied to small cluster models.[32]

In previous papers we presented preliminary results for titanozeolites[33,34] obtained with the PHF scheme. The CHA[35] structure was used as a model for zeolites, and two different compositions were considered: $X_{Ti} = 0$ and 0.5 ($X_{Ti} \equiv$ molar fraction of tetrahedral Ti). Cluster models were also considered for comparison. In ref 33, in particular, fully optimized structures were compared, and it turned out that intraframework 4-fold-coordinated Ti sites are less stable than 6-fold-coordinated sites as present in the rutile structure, and the related substitution energy was estimated at about 35 kcal·mol^{-1}. Water molecules adsorbed on Ti sites were found to have a stabilizing effect on the system.

In the present work a much larger range of framework structures and compositions is considered, and in most cases

[†] On leave from: Instituto de Tecnología Química, U.P.V.-C.S.I.C, Av. Naranjos s/n 46022 Valencia, Spain.

* To whom correspondence should be addressed.

S1089-5647(97)02343-2 CCC: $15.00
Published on Web 01/30/1998

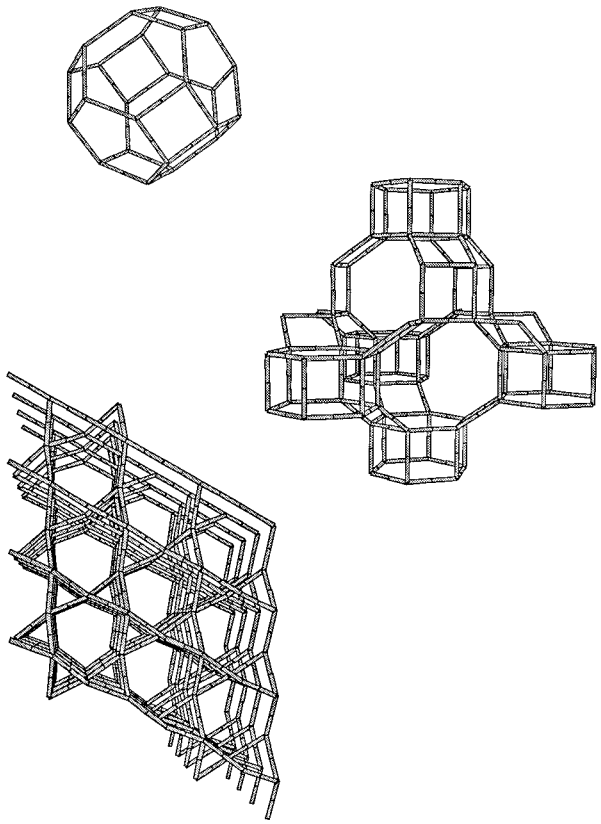

Figure 1. Framework structure of the silica models considered in this study. Only T (Si or Ti) atoms are displayed. In the case of SOD (top), a complete cubooctahedral cavity is shown. For the CHA structure (middle), one of the large cavities, the hexagonal prisms connecting them, and the characteristic 8-ring pores can be observed. The α-quartz structure (bottom) is viewed along the spiral channels.

the geometry has been fully optimized. The effect of the basis set is also discussed.

Three frameworks are considered: two, SOD[36] and CHA, have been adopted as models for zeolitic structures; the third, α-quartz[37] (QUA), has been used for comparison purposes, because it is the most stable SiO_2 polymorph and because, owing to the particular packing of the TO_4 tetrahedra, its crystalline structure is much denser than that of zeolites. SOD's framework is obtained by linking truncated cubooctahedral units called sodalite units (see Figure 1). Sodalite cavities have molecular size, and pores limited by 6-rings[12] permit the diffusion of small molecules throughout the crystal. SOD is the simplest member of the so-called sodalite family, containing other relevant members such as FAU or LTA. CHA's (chabazite) structure is an example of a more open framework, since larger cavities are connected by 8-ring pores[12] (see Figure 1). With respect to frameworks that are more interesting from the catalytic point of view, such as MFI, MEL, and *BEA,[2,4] SOD and CHA are computationally very convenient, because they have a relatively small unit cell (12 SiO_2 units) and high symmetry. This feature permits one to fully optimize the geometry of the Ti-doped compounds and then to properly account for the small energy differences between the various types of Ti centers.

2. Models and Method

For each of the three frameworks considered here, that is, SOD, CHA, and QUA, different models have been obtained by combining TiO_4 and SiO_4 units in the structure. At the limit of null Ti content, pure silica models have also been considered.

TABLE 1: Space Group Symbol, Number of Atoms per Cell (N_{at}), Composition of the Asymmetric Unit (asymm), Number of Independent Cell Parameters (M_{cell}), and Fractional Coordinates (M_{coords}) for the Various Models

	X_{Ti}	space group	N_{at}	asymm	M_{cell}	M_{coords}
rutile	1	$P4_2/mnm$	6	TiO	2	1
QUA	0	$P3_221$	9	SiO	2	4
	1/3	$C2$	9	$TiSiO_3$	4	13
SOD	0	$I\bar{4}3m$	18	SiO	1	2
	1/6	$I\bar{4}$	18	$TiSi_2O_3$	2	12
	1/3	$I\bar{4}2m$	18	$TiSiO_2$	2	6
	1/2	$P\bar{4}3n$	36	TiSiO	1	3
	1	$I\bar{4}3m$	18	TiO	1	2
CHA	0	$R\bar{3}m$	36	SiO_4	2	9
	1/2	$R\bar{3}$	36	$TiSiO_4$	2	18

Among the possible combinations of Si and Ti centers in a given framework, those corresponding to relatively high symmetry structures have been preferred, because symmetry drastically reduces the computational cost of PHF calculations in both the integral[38] and the self-consistent part of the procedure.[39]

The adopted models and their most important structural characteristics are summarized in Table 1. Five different Ti concentrations have been considered with the SOD framework, namely, $X_{Ti} = 0$, 1/6, 1/3, 1/2, and 1. The lattice is tetragonal in the $X_{Ti} = 1/3$ and 1/6 cases and cubic in all the other cases. The conventional and primitive cells contain 36 and 18 (36 in the $X_{Ti} = 1/2$ case) atoms, respectively. As regards the distribution of TO_4 groups in the frameworks, in all cases but $X_{Ti} = 1$ first neighbors of Ti are Si atoms. For $X_{Ti} = 1/2$, Ti and Si atoms alternate, and all O atoms are involved in TiOSi bridges. When $X_{Ti} = 1/3$ and 1/6, both SiOSi and SiOTi bridges occur. The number of independent geometrical parameters in the unit cell (see M_{cell} and M_{coords} in Table 1) increases from 3 to 14 as the symmetry decreases.

For the CHA framework, two models have been considered, corresponding to $X_{Ti} = 0$ and 1/2. In both cases the lattice is rhombohedral; a mirror plane is lost in the latter case with respect to the former. For $X_{Ti} = 1/2$, Ti and Si tetrahedra alternate, as in the SOD case; 18 independent coordinates must be considered in geometry optimization, since no symmetry relations occur between the coordinates of the six atoms belonging to the asymmetric unit.

As regards the QUA structure, models with $X_{Ti} = 0$ and 1/3 have been considered. In the latter case the unit cell is monoclinic (four parameters in the unit cell) and the point symmetry reduces to C_2. Rutile (TiO_2) has also been considered for comparison purposes.

Different basis sets have been used in the present study. The smallest one (BS1) consists of a standard 6-21G contraction for O atoms,[40] an 86411/411/3 (s/p/d) contraction for Ti,[41] and a modified 6-21G* for Si (the most external exponent was optimized for silicates, $\alpha = 0.13$ bohr^{-2}; for the single Gaussian d shell $\alpha_a = 0.5$ bohr^{-2} was used). This basis set performs quite well in the geometry optimization of tetrahedrally coordinated semicovalent structures, such as SOD/$X_{Ti} = 0$ and $X_{Ti} = 1/2$, as is shown in Table 2, and has been used in previous studies for the structure optimization of large unit cell SiO_2 systems.[42,43] However, in the case of fully ionic compounds such as rutile TiO_2, the 6-21G basis for oxygen is not sufficiently flexible and provides bond lengths that are too short by about 2% with respect to experiment (see Table 2). For this reason a second basis set, BS2, has been used, where the O atom is described by a 6-311G*[44] set (Ti and Si sets as in BS1). The exponents of the two most diffuse oxygen functions have been optimized and turn out to be very similar in the three different

TABLE 2: Basis Set Dependence of Selected Optimized Geometrical Parameters of Rutile and SOD, $X_{Ti} = 0$, 1/2 (distances in Å, angles in deg). In BS2m d Functions on Oxygen Have Been Dropped with Respect to BS2

	rutile			SOD/$X_{Ti} = 0$	SOD/$X_{Ti} = 1/2$	
	$r_{TiO_{ap}}$	$r_{TiO_{eq}}$	$\theta_{O_{eq}TiO_{eq}}$	r_{SiO}	r_{SiO}	r_{TiO}
BS1	1.931	1.926	99.7	1.598	1.615	1.780
BS2m	1.963	1.961	100.4			
BS2	1.978	1.951	100.0	1.607	1.618	1.792
obs[a]	1.976	1.946	98.8			

[a] Reference 45.

chemical situations of interest: systems with only Si and O atoms, systems with only Ti and O atoms, and systems with Si, Ti, and O atoms (0.905 and 0.265; 0.883 and 0.261; 0.889 and 0.279 bohr^{-2}, respectively).

BS2 provides much better bond lengths and angles than BS1 in the TiO_2 case, whereas for the SOD compounds the differences are much smaller. Table 2 also shows that, in order to correctly reproduce the difference between apical and equatorial Ti−O bond lengths,[45] d functions on oxygen are mandatory.

As calculations performed employing BS1 are considerably less demanding in computational time and disk space than when BS2 is used, geometry optimizations in all but TiO_2 cases have been carried out with BS1. On the other hand, substitution energies are much more affected than geometries by the basis set choice, because the three involved systems (rutile, pure Si zeolite, Ti−Si zeolite; see below for the definition of substitution energy) must be described by a basis set of about the same variational quality, and this is not the case with BS1, as shown above. For this reason, substitution energies have been calculated with a basis set slightly improved with respect to BS2, which we will indicate as BS2′, the only difference being that the 3G contraction for the titanium d shell becomes a 2/1G contraction. The substitution energy for CHA at the BS1 level was about 35.0 kcal·mol^{-1}[33] and drops to 19.8 and 18.6 kcal·mol^{-1} at the BS2 and BS2′ levels, respectively.

Further improvements in the basis set (additional d shells on the three atoms, addition of a diffuse sp shell on Ti, further split of the oxygen valence basis) alter the substitution energy by less than 1 kcal·mol^{-1}.

Geometry optimization has been carried out by means of a modified Polak−Ribiere algorithm[46] in which gradients are evaluated numerically. This method provides well-optimized geometries with a small number of energy points, if the potential energy well around the minimum is sufficiently wide and deep. The heaviest part of each optimization cycle is the gradient calculation, because for each derivative two energy points are required. For an N-parameters optimization and assuming that N cycles are required for the full process,[46] the computational cost is about $2N^2$ times the cost of the single PHF calculation.

Geometries have been optimized by minimizing the total energy with respect to all symmetry-independent parameters; the only exception is QUA/$X_{Ti} = 1/3$, where the cell has been constrained to keep the trigonal symmetry, in spite of a possible relaxation to a monoclinic lattice. Changes in geometry and stability produced by this additional relaxation are expected to be negligible in such a flexible structure as QUA. SOD/$X_{Ti} = 1/3$, which is more rigid than QUA, provides an example of the additional relaxation effects due to the cell symmetry reduction. When the system is allowed to relax from cubic to tetragonal symmetry, negligible changes in bond length and angles are observed; the cell volume changes by 0.2 Å^3, and the additional relaxation energy is as small as 0.8 mhartree per primitive cell.

As regards the truncation of the Coulomb and exchange series, standard computational conditions as suggested in the CRYSTAL code manual[27] have been used. For SOD and CHA, four reciprocal space k-points have been used, corresponding to a shrinking factor $S = 2$ (if $S = 4$ is used, the total energy differs at most by 3×10^{-6} hartree per cell with respect to the $S = 2$ case energies). For QUA and rutile, $S = 3$ and 8 have been used, which provide the same level of accuracy.

3. Results and Discussion

3.1. Optimized Structures. The most important optimized parameters of the titanosilica models are reported in Table 3, together with ΔV, the cell volume change per Ti atom, and α_d, the cell dilatation coefficient. Only the independent cell parameters are listed, that is, a for cubic, a and c for tetragonal or trigonal, and a and γ for rhombohedral lattices.

As regards the internal geometry parameters, that is, bond lengths and bond angles, only mean values are listed for TO distances and TOT angles (T = Si or Ti), since dispersion is negligible in most cases. In the case of OTO angles, minimum and maximum values for each system are given.

Generally speaking, the optimized bond lengths are in good agreement with previously reported data. Calculated TiO distances (see Table 3) compare quite well with accurate XRD determinations on octasiloxyspiro titanates,[47] which give an experimental TiO distance of 1.78 ± 0.01 Å for tetrahedrally coordinated Ti in a siloxy environment, a situation which is chemically similar to that in titanozeolites. This good agreement with observed TiO distances could be a consequence of cancellation of (small) errors, since the underestimation of bond distances obtained by using the BS1 basis set (about 0.5%, see previous section) in the optimization process is compensated by the systematic overestimation that is characteristic of the Hartree−Fock approach.

Measurements performed on titanozeolites using EXAFS spectroscopy give distances that range from 1.80 ± 0.01 to 1.88 ± 0.02 Å,[19,48] but in this case the actual situation of Ti atoms in the framework is controversial since either hydrated or partially hydrolyzed centers with some broken TiOSi bridges, together with extraframework TiO_2 groups, can occur.[18,49] In any of these cases Ti−O bond lengths are expected to differ from perfect framework TiO_4 centers and cannot be compared with the results presented in this work.

Previous theoretical calculations on cluster models provided values slightly larger (1.80[29] and 1.79[31] Å) than those reported here. Differences can be attributed, at least partially, to the fact that small clusters do not take properly into account the actual framework structural constraints. This point has been discussed in a previous study,[34] where it has been shown that, when a Ti atom is in a zeolitic tetrahedral position, a rather complex force field, which is not properly modeled in small clusters, acts on the TiO_4 group and its neighbors.

As regards the optimized SiO distances, mean values range from 1.60 to 1.62 Å (see Table 3). Dispersion with respect to mean values is very small, the exception being the SOD/$X_{Ti} = 1/6$ case, where, because of the low symmetry (point group S_4), there are five nonequivalent SiO bonds, whose lengths range from 1.59 to 1.63 Å. This indicates that each bond is affected in a different way by structural strains. In fact, while relatively large Ti concentrations permit homogeneous structure deformations from the pure silica models, in this case, where Ti sites are virtually isolated, a more complex distortion is produced,

TABLE 3: Selection of Optimized Geometrical Parameters of Titanosilica Models[a]

	QUA		SOD					CHA	
X_{Ti}	0	1/3	0	1/6	1/3	1/2	1	0	1/2
a	4.94	5.12	8.89	9.10	9.29	9.50	10.00	9.36	9.94
c/γ	5.43	5.56		9.19	9.39			94.7	94.7
ΔV		11.9		29.2	26.9	25.8	24.7		26.7
α_d		0.310		0.499	0.459	0.440	0.422		0.394
$\langle r_{SiO}\rangle$	1.62	1.62	1.60	1.61	1.61	1.62		1.61	1.62
$\langle r_{TiO}\rangle$		1.78		1.77	1.78	1.78	1.78		1.79
$\langle\theta_{TOT}\rangle$	144	147	160	161	162		165	152	
$\langle\theta_{TOT'}\rangle$		142		158	163	162			154
θ_{OSiO}	108	107	109	107	106	108		107	107
	112	113	110	113	111	110		111	112
θ_{OTiO}		107		106	107	106	106		105
		115		111	110	111	111		115

[a] a and c are lattice parameters, γ is the angle of the rhombohedral lattices. ΔV is the volume change per Ti atom with respect to the corresponding silica analogue, $\Delta V = [V - V_{X_{Ti}=0}]/N_{Ti}$. α_d is the cell dilatation coefficient and is defined as $\alpha_d = \Delta V \delta_{X_{Ti}=0}$, where $\delta_{X_{Ti}=0}$ is the framework density of the pure silica analogue. $\langle r_{XO}\rangle$ are mean bond lengths, $\langle\theta_{TOT}\rangle$ and $\langle\theta_{TOT'}\rangle$ are mean values of the angle (Ti or Si on both sides in the first case, one Ti and one Si in the second); distances in Å, angles in deg.

which generates locally strained situations. A second possible source of distortion might be the symmetry imposed to the model, which could prevent full structure relaxation.

In all cases the OTO angles deviate significantly from the regular tetrahedral value. Deviations for T = Ti are always larger than for T = Si. This is consistent with the fact that SiO bonds, owing to their larger covalent character, are more directional than TiO bonds; the quite ionic nature of the latter suggests that the geometry of the TiO_4 tetrahedra is determined also by ion-packing requirements. As regards the TOT angles, no relevant changes are observed when substituting Si by Ti, either within the TOT bridge or in the nearest neighbors. This seems to indicate that TOT angles mainly depend on the topology of the structure, while they are almost independent of the nature of the T cation.

Substitution of a Si by a Ti atom in the framework always results in an increase of the cell volume (see Table 3). This effect is well-known for titanozeolites and is used for evaluating the Ti content of the samples, since a linear relation between X_{Ti} and cell volume has been found in the range of small X_{Ti} in titanosilicalites.[49] The proportionality constant of such a relation, α_d, has been found to be 0.395 for TS-1.[49] Thangaraj et al.[50] reported a smaller value for α_d of TS-1 (0.308). However, as proposed in ref 49, the discrepancy might come from the existence of extraframework Ti atoms in the used samples, which are expected to cause minor or null cell expansions.

As a first order approximation, a relatively constant ΔV (see definition in the footnote of Table 3) might be assumed for different Ti concentrations and frameworks. This is however not the case when a wide range of X_{Ti} and structures are considered. The largest difference is observed between zeolitic structures and α-quartz. In the former, ΔV ranges from 24.7 to 29.2 Å^3, whereas in the latter (QUA/X_{Ti} = 1/3) it is about 11.9 Å^3. This difference is not related to important differences in TO distances or TOT angles between α-quartz and titanozeolite models; rather, it must be attributed to the packing of the TO_4 tetrahedra in each structure. In the case of α-quartz tetrahedra are linked to form spiral channels that provide high flexibility to the structure; such a flexibility is, on the contrary, absent in the case of zeolites, where the framework is built by linking more rigid subunits.[12,13]

As regards the influence of the Ti content on ΔV, the results obtained for the SOD framework (see Table 3) indicate that the lower the Ti content, the larger ΔV. This can be explained in terms of better ion packing for TiO_4 than for SiO_4 tetrahedra, owing to the more ionic character of the former (see discussion above); structures with higher Ti concentration can therefore reach a more compact arrangement. It is to be stressed that changes in ΔV (and consequently in α_d) are expected to be negligible for the narrow range of X_{Ti} values where the linear relation between Ti content and cell volume is currently assumed.

TABLE 4: Calculated Total (E_{PHF}, in Hartree) and Substitution (ΔE_{Subs}, in kcal·mol^{-1}) Energies for All the Optimized Structures[a]

	X_{Ti}	E_{PHF}	ΔE_{Subs}
rutile	1	−1996.7629	
QUA	0	−1316.7826	
	1/3	−1876.2060	19.2
SOD	0	−2633.5551	
	1/6	−3192.9720	24.3
	1/3	−3752.4122	17.0
	1/2	−8623.6772	17.4
	1	−5990.0930	20.5
CHA	0	−5267.0965	
	1/2	−8623.6595	18.6

[a] Differences between the $X_{Ti} = 0$ data indicate that pure silica QUA is more stable than pure silica SOD and CHA by 1.1 and 1.8 kcal·mol^{-1} per SiO_2 unit, respectively.

3.2. Energies and Relative Stabilities. The total energy of the various structures evaluated with BS2′ at the geometry optimized with BS1 (BS2 for TiO_2) is given in Table 4. The substitution of a silicon by a titanium atom in the framework can be modeled by the following reaction:

$$\left(\frac{1-x}{x}\right)SiO_2[FT] + TiO_2[rutile] \rightarrow (SiO_2)_{(1-x)/x}(TiO_2)[FT] \quad (1)$$

where FT stands for the framework type (SOD, CHA, or QUA). Using eq 1 and the PHF energies, the relative stability of titanosilicas with respect to pure silica and TiO_2 can be estimated. Table 4 lists the calculated reaction energies, ΔE_{Subs}, for eq 1.

Reaction 1 is endothermic, and ΔE_{Subs} ranges from 17 to 24 kcal·mol^{-1}, the actual value changing as a function of framework and composition. At high Ti concentration, SOD is the framework that requires the lowest energy to form titano compounds, whereas QUA is at the other extreme. This order not only reflects the stability scale of the titano compounds but is also a consequence of the relative stability of the pure silica analogues (QUA is 1.1 and 1.8 kcal·mol^{-1} per SiO_2 unit more stable than SOD and CHA, respectively).

TABLE 5: Mean Atomic Net Charges, $\langle Q_A \rangle$, and Mean Bond Population, $\langle P_{AB} \rangle$, for All Models, Calculated by Using the Mulliken Partition of the Electronic Density

	X_{Ti}	$\langle Q_{Si} \rangle$	$\langle Q_{Ti} \rangle$	$\langle Q_O \rangle$	$\langle P_{OSi} \rangle$	$\langle P_{OTi} \rangle$
rutile	1		+2.87	−1.44		0.032
QUA	0	+1.78		−0.89	0.323	
	1/3	+1.94	+2.61	−1.06	0.298	0.069
SOD	0	+1.67		−0.84	0.339	
	1/6	+1.88	+2.58	−0.99	0.311	0.068
	1/3	+1.87	+2.60	−1.03	0.315	0.071
	1/2	+1.90	+2.60	−1.13	0.314	0.071
	1		+2.63	−1.31		0.055
CHA	0	+1.72		−0.86	0.335	
	1/2	+1.91	+2.60	−1.13	0.311	0.071

The dependence of substitution energy on Ti concentration can be studied from the results obtained for the SOD framework. For the three highest X_{Ti} models, ΔE_{Subs} increases with X_{Ti}. At the lowest Ti concentration ($X_{Ti} = 1/6$), however, ΔE_{Subs} is the highest of the series. This can be explained by structural features, since, as stated above, this model shows SiO_4 tetrahedra slightly distorted with respect to the normal silica structure as a result of the strains generated by the TiO_4 site in the framework and, probably, of the symmetry constraints imposed on the model.

3.3. Electronic Structure. Mean atomic charges and bond populations, obtained from a Mulliken analysis, are given in Table 5. Charges on Ti atoms are about $+0.7|e|$ larger than those on silicon atoms, and TiO bond populations about 5 times smaller than SiO ones in titanosilicas. This is consistent with the mean O atomic charges, which increase as the Ti content increases, and is to be attributed mainly to the higher ionicity of the TiO bond with respect to SiO.

A sort of global increase of the ionicity with increasing X_{Ti} is also observed, since the larger the Ti content of a given model is, the larger are the mean charges on Ti and Si atoms.

The density of states (DOS) for SOD/$X_{Ti} = 0$, 1/2, and 1 is plotted in Figure 2. Valence electrons are distributed in two main bands. The lowest is a nearly pure oxygen 2s band, and the highest is mostly an oxygen 2p band, with small contributions from Ti and Si, as shown by the projected DOS. In the $X_{Ti} = 1/2$ case the O 2p band shows a clear division into two narrow and one wide sub-bands, which are not easy to assign, whereas in the $X_{Ti} = 0$ and 1 cases, only one narrow sub-band is observed. Ti and Si projected DOS show that both cations contribute almost equally to all the sub-bands of the $X_{Ti} = 1/2$ case. The double peak can be interpreted as due to the strong interaction of TiO and SiO states (that in pure TiO_2 and SiO_2 systems generates a single peak) in TiOSi bridges.

The first virtual band of 4-fold-coordinated Ti-containing systems is mostly contributed by Ti 3d orbitals. This band is very important, because it is the one involved in interactions when Ti sites act as electron acceptors, as is supposed to occur in reactions catalyzed by titanozeolites. It should be noticed that this band is only marginally influenced by the chemical nature of the first neighbors (Ti or Si) of the TiO_4 sites.

3.4. Character of the TiO Bond in Titanozeolites. In this section we shall consider the peculiar characteristics of the TiO bond, when Ti is 4-fold-coordinated and is merged in a silica environment. TiO bonds in titanozeolites are significantly shorter than in the case of rutile, as results from Tables 2 and 3. This is a consequence of the different ion packing resulting from 4- and 6-fold coordination of Ti. In both cases the TiO bond can be characterized as essentially ionic; in the 4-fold coordination, however, the shorter distance permits some additional electronic interaction, which can be interpreted as an increase of the covalent character of the bond. Population analysis data listed in Table 5 seem to support this hypothesis, as TiO bond populations in titanosilicas are larger than in rutile, while atomic charges on Ti and O are smaller.

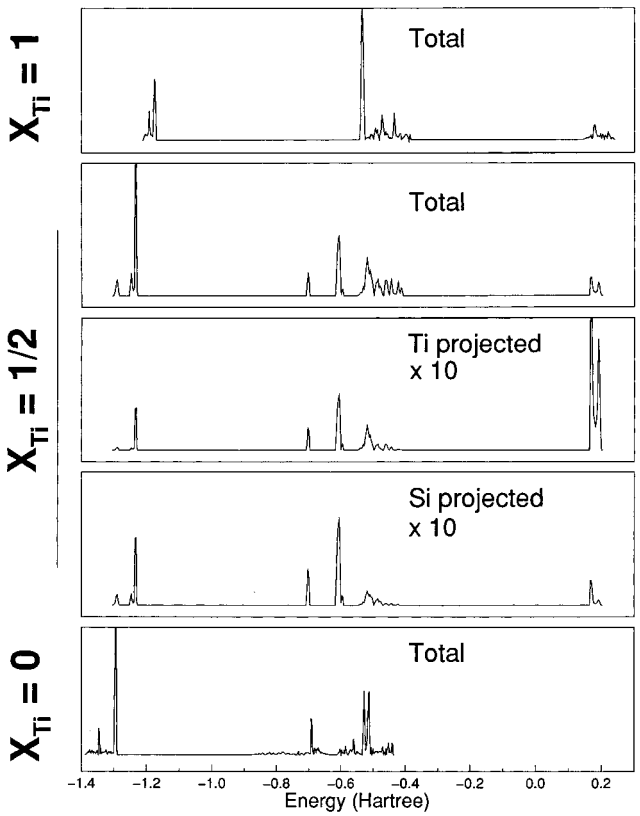

Figure 2. Density of states (DOS) for the SOD/$X_{Ti} = 0$, 1/2, and 1 models. Arbitrary units have been used for the total DOS. Projected DOS have been multiplied by a factor 10.

Optimized bond lengths are very similar in all the considered titanosilica models (Table 3). Differences are small and within the limit of accuracy of the numerical optimization method. Nevertheless, when the Ti content increases, a trend toward larger TiO and SiO distances is observed for the three types of structures. A similar behavior has been observed for cluster model calculations when comparing SiO distances in systems with and without Ti.[31] Such an increase of the bond lengths is connected with the similar trend of ionicities observed from atomic charges (see discussion above), indicating that the general covalent character of the system decreases while increasing the Ti content.

Additional information on the electronic structure of Ti atoms in 4- and 6-fold coordination can be obtained by the difference (bulk minus superposition of ionic charges) electron density maps (Figure 3). In the rutile figure (top), apart from the usual shrinkage of the ionic charge as a consequence of electrostatic effects and short-range repulsion, the main feature is the back-donation (with respect to the fully ionic representation: Ti^{4+} and O^{2-}) from oxygen to titanium diffuse d orbitals. In the SOD/$X_{Ti} = 1$ figure (bottom), more important changes with respect to the ionic situation are observed. The usual contraction of the oxygen density is observed in the direction perpendicular to the TiO bond, whereas along the bond a noticeable buildup of charge takes place. The electrons transferred to Ti atoms are not concentrated along the line connecting the Ti and O atoms, as was the case of rutile; on the contrary they are displaced in the opposite direction, in order to minimize the repulsion with O electrons. The reduced overall electrostatic

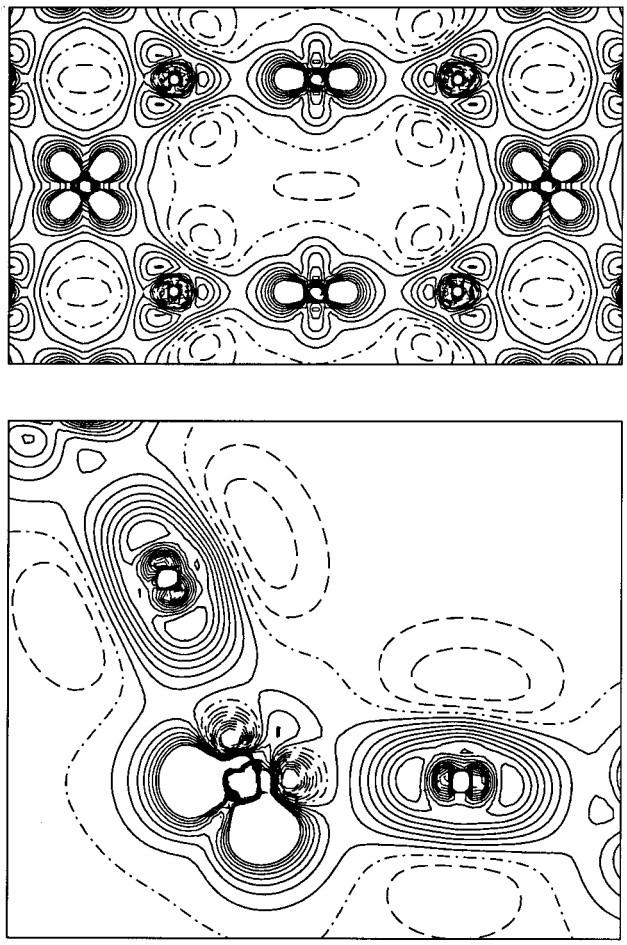

Figure 3. Difference electron density maps for rutile (top) and SOD/$X_{Ti} = 1$ (bottom). Plots are obtained by subtracting from the periodic charge density the superposition of spherical ionic charges, obtained with the same basis set used for the bulk calculation. Isodensity lines differ by $0.005e \times \text{bohr}^{-3}$. Continuous, dashed, and dot-dashed lines correspond to positive, negative, and zero differences, respectively. For rutile, the map refers to the (001) plane containing four Ti (on the two principal axes of the picture) and four O atoms. For the bottom figure, the selected plane is the one containing a single OTiO group.

effects (volumes are 83.2 and 31.2 Å^3 per TiO_2 unit for SOD/$X_{Ti} = 1$ and rutile, respectively) and the need of reducing the electron repulsion in the shorter TiO bonds are at the origin of the lowest stability of SOD/$X_{Ti} = 1$ with respect to rutile (20 kcal·mol^{-1} per TiO_2 unit; see Table 4).

In Figure 4 electron density difference maps for SOD/$X_{Ti} = 1/2$ are reported. The top one (the reference is a superposition of spherical ionic charges) is similar to the corresponding one for SOD/$X_{Ti} = 1$, indicating that the character of the TiO bond in 4-fold coordination does not change very much when changing the Ti concentration. However, when considering the bottom plot, where the difference between $X_{Ti} = 1/2$ and 1 is given, it turns out that the polarization of oxygen atoms decreases as one Ti of the bridge is substituted by a Si atom, as a result of the reduced electric field in the OSi bond direction. This feature, together with the charge transfer from O to Si in order to form the SiO bond, decreases the repulsion between the electrons in the TiO bond and those in the Ti d shell, observed for the SOD/$X_{Ti} = 1$ case, and permits the partial relaxation of the electron density around the Ti atoms.

Such a complex interaction between TiO and SiO bonds may be the main result of the mixed Ti−Si participation in the DOS diagram of SOD/$X_{Ti} = 1/2$ discussed above (see Figure 2). The larger stability of titanosilicas with respect to pure tetrahedrally

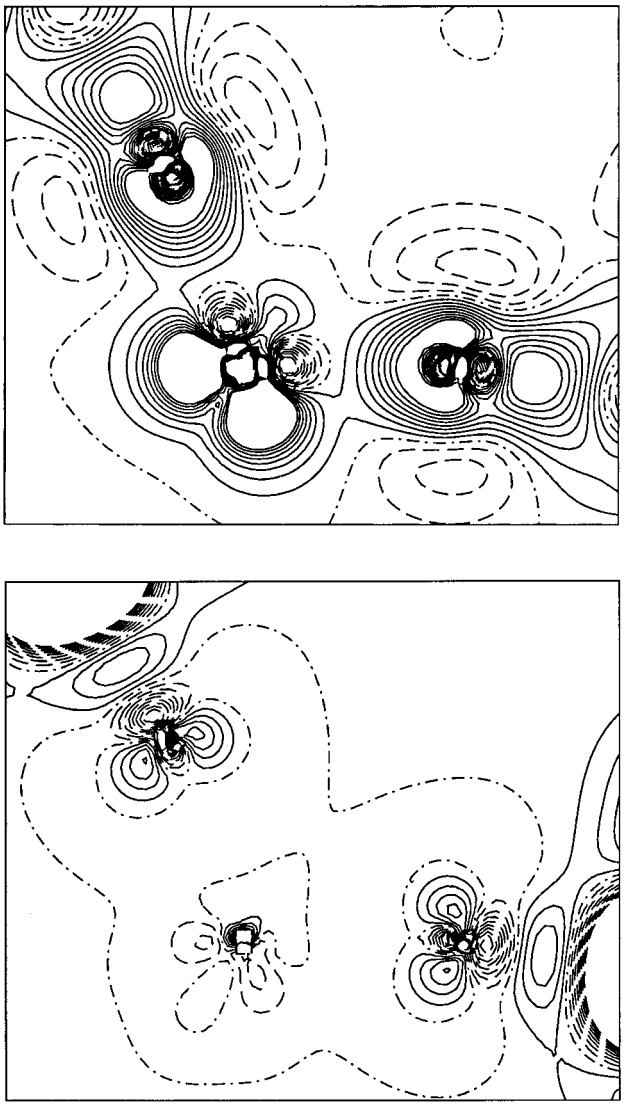

Figure 4. Difference electron density maps for SOD/$X_{Ti} = 1/2$. Maps are obtained by subtracting from the periodic charge density the superposition of spherical ionic charges (top) or the density of SOD/$X_{Ti} = 1$ (bottom). In the latter case the geometry of the $X_{Ti} = 1$ model was constrained to match the geometry of $X_{Ti} = 1/2$. Scale and symbols as in Figure 3.

linked TiO_2 seems to be connected to such an influence of the silica environment on the electronic structure of the Ti sites.

4. Concluding Remarks

The introduction of Ti atoms into a tetrahedral site of siliceous zeolites involves important changes in the crystal geometry that are mainly due to the increase of the TO bond length from about 1.61 to 1.79 Å. The most evident effect is the increase of the cell volume. However, the volume change per Ti site, ΔV, largely depends on the framework type considered, as the structural response in each case involves different ways of tetrahedra packing. A dependence of ΔV on the Ti content is observed from our results, but very large X_{Ti} changes are required in order to obtain non-negligible ΔV differences. Since, at the moment, the synthesis of titanozeolites can be carried out within a very narrow X_{Ti} range (≤ 0.03), in practice the use of the overall increase of the cell volume as a measure of the Ti content of a given titanozeolite is supported by our calculations.

The substitution of a Si by a Ti atom in a zeolite framework is an endothermic process, when evaluated with respect to pure

silicozeolites and rutile, the reaction energy ranging between 17 and 24 kcal·mol^{-1} per Ti atom. This means that the formation of zeolitic Ti sites is thermodynamically less favored than the formation of extraframework TiO_2 clusters in the cavities and explains the difficulty of synthesizing high Ti content zeolites. Nevertheless, the fact that some content of intraframework Ti can be obtained indicates that the synthesis is conditioned not only by thermodynamics and that kinetic effects can play a relevant role in the reaction. In particular, it has been suggested[33] that the initial formation of hydrated Ti sites, in which the coordination can be either 5- or 6-fold, favors the inclusion of Ti atoms in the framework. A theoretical study concerning the relevance of water adsorption in stabilizing zeolitic Ti sites is in progress.

As a consequence of the large difference between the size of SiO_4 and TiO_4 tetrahedra, frameworks show distortions around the Ti sites with respect to the pure silicozeolite, which are larger in models with low Ti content. It is to be stressed that the structural effect of the substitution propagates beyond the first neighbors, as the geometry of the second neighbors' SiO_4 tetrahedra are also rather affected in the studied models. In particular, when Ti sites are on average far from each other, a nonhomogeneous lattice distortion is observed that yields a higher substitution energy with respect to the high Ti content case. This suggests that, even if a low overall Ti concentration can be achieved by synthesis, a distribution having sparse zones with relatively high local density of Ti sites might be energetically favored. This effect is conditioned by the capacity of the zeolitic framework to assimilate the deformations produced by the inclusion of Ti atoms.

As a final comment, from this study it turns out that the framework composition plays a limited role in the electronic properties of Ti sites. When Ti centers are surrounded only by Si atoms, as, for instance, in models with $X_{Ti} = 1/2$, where the two kinds of centers alternate, sites are estimated to be only 3.1 kcal·mol^{-1} more stable than in pure TiO_2 frameworks. This difference is to be attributed to a certain amount of reciprocal perturbation between the electrons involved in the TiO and SiO bonds of the same TiOSi bridge. On the other hand, no relevant differences in the electronic properties are observed when reducing X_{Ti} to values lower than 1/2; this indicates that, apart from structural features, Ti atoms that do not belong to first-neighbor tetrahedra essentially do not interact. This information is useful to design efficient periodic models for the study of the catalytic behavior of titanozeolites, because it indicates that symmetric models with high Ti content can be considered where no relevant interactions between active centers are to be expected.

Acknowledgment. C.Z. thanks the Spanish "Ministerio de Educación y Ciencia" for a postdoctoral grant. R.D. thanks Italian CNR and "Ministero dell'Università e della Ricerca Scientifica e Tecnologica (MURST)" for financial support.

References and Notes

(1) Taramasso, M.; Perego, G.; Notari, B. U.S. Patent 4,410,501, 1983.
(2) Perego, G.; Bellusi, G.; Corno, C.; Taramasso, M.; Buonomo, F.; Esposito, A. New developments in zeolite science and tecnology. In *Studies in Surface Science and Catalysis*; Murakami, Y., Ijima, A., Ward, J., Eds.; Elsevier: Amsterdam, 1986; Vol. 28, p 129.
(3) Bellusi, G.; Carati, A.; Clerici, G. M.; Esposito, A.; Millini, R.; Buonomo, F. Belg. Patent 1,001,038, 1989.
(4) Camblor, M. A.; Corma, A.; Martínez, A. *J. Chem. Soc., Chem. Commun.* **1992**, 589.
(5) Camblor, M. A.; Corma, A.; Perez-Pariente, J. *Zeolites* **1993**, *13*, 82.
(6) Ferrini, C.; Kouwenhoven, H. W. In *New Developments in Selective Oxidation*; Cento, G., Trifirò, F., Eds.; Elsevier: Amsterdam, 1990; p 53.
(7) Kim, G. J.; Cho, B. R.; Kim, J. H. *Catal. Lett.* **1993**, *22*, 259.
(8) Blasco, T.; Corma, A.; Navarro, M. T.; Perez-Pariente, J. *J. Catal.* **1995**, *156*, 65.
(9) Anderson, M.; Terasaki, O.; Ohsina, T.; Philippou, A.; Mackay, S.; Ferreira, A.; Rocha, J.; Lidin, S. *Nature* **1994**, *367*, 347.
(10) Tanev, P. T.; Chibwe, M.; Pinnavaia, T. J. *Nature* **1994**, *368*, 321.
(11) Szostak, R. *Molecular Sieves; Principles of Synthesis and Identification*; Van Nostrand-Reinhold: New York, 1989.
(12) Meier, W. M.; Olson, D. H. *Atlas of Zeolites Structure Types*; Butterworth: London, 1992.
(13) Smith, J. V. *Chem. Rev.* **1988**, *88*, 149.
(14) Boccuti, M. R.; Rao, K. M.; Zecchina, A.; Leofanti, G.; Petrini, G. Structure and Reactivity of Surfaces. In *Studies in Surface Science and Catalysis*; Morterra, C., Zecchina, A., Costa, G., Eds.; Elsevier: Amsterdam, 1988; Vol. 48, p 133.
(15) Tuel, A.; Diab, J.; Gelin, P.; Dufoux, M.; Dutel, J. F.; Ben Taarit, Y. *J. Mol. Catal.* **1990**, *63*, 95.
(16) Notary, B. *Catal. Today* **1993**, *18*, 163.
(17) Berger, S.; Bock, W.; Marth, C.; Raguse, B.; Reetz, M. *Magn. Reson. Chem.* **1990**, *28*, 559.
(18) Blasco, T.; Camblor, M. A.; Corma, A.; Pérez-Pariente, J. *J. Am. Chem. Soc.* **1993**, *115*, 11806.
(19) Pei, S.; Zajac, G.; Kaduk, J.; Faber, J.; Boyanov, B.; Duck, D.; Fazzini, D.; Morrison, T.; Yang, D. *Catal. Lett.* **1993**, *21*, 333.
(20) Bordiga, S.; Coluccia, S.; Lamberti, L.; Marchese, L.; Zecchina, A.; Boscherini, F.; Buffa, F.; Genoni, F.; Leofanti, G.; Petrini, G.; Vlaic, G. *J. Phys. Chem.* **1994**, *98*, 4125.
(21) Lopez, A.; Tuilier, M.; Guth, J.; Delmotte, L.; Popa, J. *J. Solid State Chem.* **1993**, *102*, 480.
(22) Trong On, D.; Bonneviot, L.; Bittar, A.; Sayari, A.; Kaliaguine, S. *J. Mol. Catal.* **1992**, *74*, 223.
(23) Deo, G.; Turek, A.; Wachs, I.; Huybrechts, D.; Jacobs, P. *Zeolites* **1993**, *13*, 365.
(24) Scarano, D.; Zecchina, A.; Bordiga, S.; Geobaldo, F.; Spoto, G.; Petrini, G.; Leofanti, G.; Padovan, M.; Tozzola, G. *J. Chem. Soc., Faraday Trans.* **1993**, *89*, 4123.
(25) Dart, C.; Khouw, C.; Li, H.-X.; Davis, M. *Microporous Mater.* **1994**, *2*, 425.
(26) Pisani, C.; Dovesi, R.; Roetti, C. Hartree-Fock Ab Initio Treatment of Crystalline Solids. In *Lecture Notes in Chemistry Series*; Springer: Berlin, 1988; Vol. 48.
(27) Dovesi, R.; Saunders, V. R.; Roetti, C.; Causà, M.; Harrison, N. M.; Orlando, R.; Aprà, E. *CRYSTAL95 User Documentation*; Università di Torino: Torino, 1995.
(28) Nicholas, J. B.; Hess, A. C. *J. Am. Chem. Soc.* **1994**, *116*, 5428.
(29) Millini, R.; Perego, G.; Seiti, K. Zeolites and Related Microporous Materials: State of the Art 1994. In *Studies in Surface Science and Catalysis*; Weikamp, J., Karge, H. G., Pfeifer, H., Hölderich, W., Eds.; Elsevier: Amsterdam, 1994; Vol. 84, p 2123.
(30) Jentys, A.; Catlow, C. *Catal. Lett.* **1993**, *22*, 251.
(31) de Man, A. J. M.; Sauer, J. *J. Phys. Chem.* **1996**, *100*, 5025.
(32) Neurok, M.; Manzer, L. E. *J. Chem. Soc., Chem. Commun.* **1996**, 1133.
(33) Zicovich-Wilson, C. M.; Dovesi, R. *J. Mol. Catal. A: Chem.* **1997**, *119*, 449.
(34) Zicovich-Wilson, C. M.; Dovesi, R. *Nuovo Cimento*, in press.
(35) Calligaris, M.; Nardin, G.; Randaccio, L.; Comin Chiaramonti, P. *Acta Crystallogr.* **1982**, *B38*, 602.
(36) Bibby, D. M.; Dale, M. P. *Nature* **1985**, *317*, 157.
(37) Jorgensen, J. D. *J. Appl. Phys.* **1978**, *49*, 5473
(38) Dovesi, R. *Int. J. Quantum Chem.* **1986**, *29*, 1755.
(39) Zicovich-Wilson, C. M.; Dovesi, R. *Int. J. Quantum Chem.*, in press.
(40) Binkley, J. S.; Pople, J. A.; Hehre, W. J. *J. Am. Chem. Soc.* **1980**, *102*, 939. Gordon, M. S.; Binkley, J. S.; Pople, J. A.; Pietro, W. J.; Hehre, W. J. *J. Am. Chem. Soc.* **1982**, *104*, 2797.
(41) Saunders, V. R. Private communication. Reinhardt, P.; Hess, B. A.; Causà, M. *Int J. Quantum Chem.* **1996**, *58*, 296.
(42) Aprà, E.; Dovesi, R.; Freyria-Fava, C.; Pisani, C.; Roetti, C.; Saunders, V. R. *Modeling Simul. Mater. Sci. Eng.* **1993**, *1*, 297.
(43) Zicovich-Wilson, C. M.; Dovesi, R. *Chem. Phys. Lett.* **1997**, *277*, 227.
(44) Krishman, R.; Binkley, J. S.; Seeger, R.; Pople, J. A. *J. Chem. Phys.* **1980**, *72*, 650. Clark, T.; Chandrasekhar, I.; Spintznagel, G. W.; Schleyer, P. R. *J. Comput. Chem.* **1983**, *77*, 3654.
(45) Meagher, E. P.; Lager, G. A. *Can. Mineral.* **1979**, *17*, 77.
(46) Press, W. H.; Flannery, B. P.; Teukolsky, S. A.; Vetterling, W. T. *Numerical Recipes*; University Press: New York, 1989.
(47) Hursthouse, M.; Hossain, M. *Polyhedron* **1984**, *3*, 95.
(48) Trong On, D.; Bittar, A.; Sayari, A.; Kaliaguine, S.; Bonneviot, L. *Catal. Lett.* **1992**, *74*, 233.
(49) Millini, R.; Previde Massara, E.; Perego, G.; Bellusi, G. *J. Catal.* **1992**, *137*, 497.
(50) Thangaraj, A.; Eapen, M.; Sivasankar, S.; Ratnasamy, P. *Zeolites* **1991**, *12*, 943.